Hybrid linear/non-linear adaptive controller for battery charger/discharger in renewable power systems

Controlador hibrido lineal/no-lineal adaptativo para un sistema de carga/descarga de una batería en sistemas de energía renovable

C. A. Ramos-Paja[1], D. González[1], S. I. Serna-Garcés[2]

ABSTRACT

This paper presents the control of an Energy Management System (EMS) for renewable DC sources connected to the load and a battery. The EMS is aimed at improving the performance of electric systems such as electrical vehicles and stand-alone applications. This work considers a Boost converter controlled by a Maximum Power Point Tracking algorithm (MPPT) to maximize the power generation of a renewable DC source. Moreover, a battery charger/discharger, based on a bidirectional dc/dc converter, is used to control the energy flows between the generator, the battery and the load. This paper proposes a sliding-mode current controller to guarantee the global stability of the bidirectional converter, i.e. of the EMS. In addition, a digital adaptive controller is proposed to regulate the voltage of the EMS DC bus, which enables to provide a stable load voltage. Detailed simulation results validate the proposed controller.

Keywords: EMS, adaptative controller, bidirectional dc/dc converter, sliding-mode controller, renewable power systems.

RESUMEN

Este artículo presenta un sistema de administración de energía (EMS – Energy Management System) para fuentes de energía renovable DC conectada a una carga y una batería. El EMS tiene como objetivo mejorar el desempeño del sistema eléctrico en vehículos eléctricos o aplicaciones autónomas. Este trabajo considera un convertidor Boost controlado por un algoritmo para el rastreo del punto de máxima potencia con el fin de maximizar la generación de potencia DC de la fuente de energía no renovable. Por otra parte, un sistema de carga/descarga de batería basado en un convertidor DC/DC bidireccional, es utilizado para controlar el flujo de energía entre la fuente, la batería y la carga. Este artículo propone un control de corriente por modos deslizantes con el fin de garantizar la estabilidad global del convertidor bidireccional. Adicionalmente, un control digital adaptativo es propuesto para regular el voltaje del bus DC del EMS, cuyo objetivo es proveer un voltaje estable a la carga. Resultados de simulaciones validan el controlador propuesto.

Palabras clave: Sistema de administración de energía, controlador adaptativo, convertidor DC/DC bidireccional, control por modos deslizantes, energía renovable.

Introduction

Renewable energy systems are a suitable alternative for developing micro-grids for stand-alone applications. In particular, the use of fuel cells (FC) and photovoltaic (PV) modules as power sources has significantly increased due to its pollution free operation, which is a major concern nowadays (Romero-Cadaval, et al., Sept 2013). The selection of a FC or PV source depends on the application: FC systems provide uninterrupted power production when fuel is provided (Ramos-Paja, et al., June 2010), which is a major characteristic of the classical combustion engines. However, FC can operate with clean fuels such as hydrogen to avoid environmental pollution. Moreover, FC are not constrained to the Carnot limit (Ramos-Paja, et al., June 2010), hence they are much more efficient in comparison with combustion engines. In contrast, PV systems only provide energy when the sun light (irradiance) is present. Therefore, an auxiliary power source is required to support the load during nights or in step-up transients (Sun, Zhang, Xing, & Guerrero, Oct 2011) (Ramos-Paja, Bordons, Romero, Giral, & Martínez-Salamero, March 2009). However, PV systems do not require fuel storage, which is a major advantage in terms of cost. In such a way, FC systems are mainly used for critical applications such as buck-up power sources for hospitals or telecommunications and automobiles (Ramos-Paja, Bordons, Romero, Giral, & Martínez-Salamero, March 2009) (Chen, May 2014), while PV systems are used for non-critical applications such as stand-alone sources and street lights (Romero-Cadaval, et al., Sept 2013). Moreover, FC and PV generators have been combined to support critical loads with low fuel consumption (Bizon, Oproescu, & Raceanu, Jan 2015): the PV source produces the power achievable with the sun light, while the FC system produces the power in excess required by the load; hence if the PV source produces enough power the FC does not operate.

Renewable generators also require an optimization system to guarantee an efficient operation named Maximum Power Point Tracker (MPPT). In the case of PV systems the MPPT defines the operation voltage that maximizes the power produced (Romero-Cadaval, et al., Sept 2013); otherwise, despite being exposed to high sun irradiance, the PV module could produce almost no energy. A clear description of such a problem is given in (Femia,

[1] Departamento de Energía Eléctrica y Automática, Facultad de Minas, Universidad Nacional de Colombia, Medellín, CO. E-mail: {caramosp, dgonzalezm}@unal.edu.co

[2] Departamento de Electrónica y Telecomunicaciones, Facultad de Ingenierías, Instituto Tecnológico Metropolitano, Medellín, CO.
E-mail: danielgonzalez, sergioserna}@itm.edu.co

Petrone, Spagnuolo, & Vitelli, July 2005). In the case of FC systems, the requested electrical power could be produced at different current/voltage values as explained in (Ramos-Paja, Spagnuolo, Petrone, & Mamarelis, April 2014): since the hydrogen consumption is proportional to the FC current (Ramos-Paja, Bordons, Romero, Giral, & Martínez-Salamero, March 2009), then the optimal operation condition is achieved when the load power is supplied at the minimum FC current. In both FC and PV cases, the implementation of the MPPT requires two devices: a digital processor to execute the MPPT algorithm, and an unidirectional dc/dc converter to define the source voltage or current. In addition, the operation of the MPPT generates a bandwidth limitation since the transition from one optimal condition to another one is not instantaneous (Femia, Petrone, Spagnuolo, & Vitelli, July 2005) (Ramos-Paja, Spagnuolo, Petrone, & Mamarelis, April 2014), or even not possible if the sun irradiance or fuel are constrained. Moreover, since the associated dc/dc converter is controller to track the optimal operation condition, i.e. by the MPPT, such a dc/dc converter is regulated as follows: in PV systems the converter input voltage is controlled (Bianconi, et al., March 2013), while in FC systems the converter input current is regulated (Ramos-Paja, Spagnuolo, Petrone, & Mamarelis, April 2014). Therefore, the output voltage of the dc/dc converter is not regulated. Such a condition makes impossible to provide a stable operation voltage to the load.

The previous limitations have been addressed by adding a battery as depicted in **Figure 1**: in load transients the battery provides or absorbs the power difference between the generator and load profiles. Such a condition enable the system to supply any load profile, and at the same time, to store energy when the load is not consuming, or even to recover energy produced by the load, e.g. regenerative break in electrical vehicles. In addition, a bidirectional dc/dc converter (named charger/discharger) is added to interface the battery and the load with two main objectives: first, the charger/discharger is regulated to provide a stable voltage to the load; and second, the charger/discharger isolates the battery and load voltages, it making possible to use any battery for any load voltage requirement. The main problem in this kind of power systems concerns the design and control of the Energy Management System (EMS) required to regulate the power exchanged between the battery, the generator and the load. This paper proposed an EMS based on a hybrid linear/non-linear adaptive controller regulating the charger/discharger. In such a way, the charger/discharger is controlled to provide the required operation voltage to the load, and at the same time, to manage the battery power flow in agreement with the generator production and load requirement. The main challenge in such a solution is to guarantee the voltage stability in any operation condition. Moreover, since the bidirectional dc/dc converter must to manage both positive (discharge) and negative (charge) power flows, a single controller is difficult to design for both tasks. Therefore, this proposed solution combines a nonlinear controller to guarantee global stability, and an adaptive controller to ensure a consistent performance in any condition.

The paper is organized a follows: Section II presents the EMS topology and the charger/discharger circuit, Section III presents the non-linear controller designed to guarantee stability and Section IV presents the adaptive controller designed to provide an stable load voltage. Section V verifies the control system performance by means of simulation results and Section VI presents the paper conclusions.

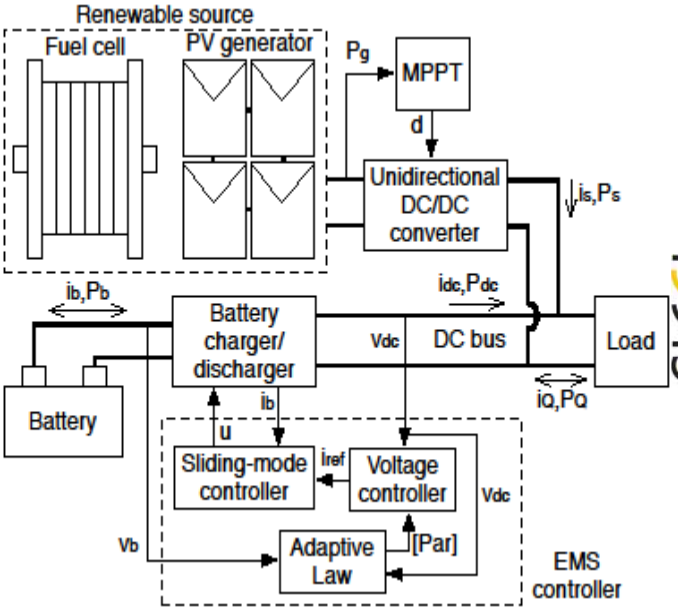

Figure 1: Hybrid fuel cell/photovoltaic power system.

Energy Management System

Figure 1presents a widely adopted structure for power systems based on renewable generators (Bizon, Oproescu, & Raceanu, Jan 2015): a generator managed by a dc/dc converter, which in turns is controlled by an MPPT controller to ensure optimal operation; and a battery interfaced with a charger/discharger, i.e. a bidirectional dc/dc converter. The outputs of both dc/dc converters are connected to form a bidirectional dc bus. Since the loads are connected to such a dc bus, then the dc/dc converters must to provide a stable voltage to the bus in any operation condition. Since the dc/dc converter associated to the renewable generator is controller to ensure an MPPT operation, the output voltage of such a dc/dc converter is not controlled. Therefore, that unidirectional dc/dc converter behaves as a power source providing the profile P_s with non-regulated current i_s. In consequence, the charger/discharger must be controlled to provide a regulated voltage v_{dc} to the dc bus. This condition implies that such a bidirectional dc/dc converter must to behave as a voltage source with a power profile equal to the difference (positive or negative) between the load and generator powers, i.e. $P_{dc} = P_Q - P_s$ and $i_{dc} = i_Q - i_s$ since v_{dc} is controlled.

The bidirectional dc/dc converter, i.e. charger/discharger, must be implemented with synchronous structures (Jang & Agelidis, May 2011) to enable both positive and negative current flows from/to the battery. A classical structure used for such an application is the bidirectional topology presented in Figure 2, which interfaces common low-voltage batteries v_b with high-voltage dc buses v_{dc}, i.e.$v_b < v_{dc}$. In such an electrical scheme the battery is modeled by a voltage source v_b with current i_b, while the dc bus is modeled by a capacitor C_{dc} and a current source i_{dc}. Such a model makes possible to account for step load transients, both positive or negative. Moreover, the Mosfets of the dc/dc converter are complementary controlled with the signal u: when $u = 1$ the vertical Mosfet is turned ON and the horizontal Mosfet is turned OFF, when $u = 0$ the vertical Mosfet is turned OFF and the horizontal Mosfet is turned ON.

As previously described, the main challenge in this system concerns to guarantee the voltage stability: the non-linear nature of the dc/dc converter makes impossible to guarantee global stability using a classical lineal controller; in addition, a single controller must be designed to control the converter in both positive and negative power flows, which is not a trivial task. Several authors have recognized such a drawback of the linear controllers, using non-linear controllers to guarantee global stability on dc/dc converters, e.g. (Bianconi, et al., March 2013), (Zhao, Qiao, & Ha, March 2014), (Inthamoussou, Pegueroles-Queralt, & Bianchi, Sept 2013).

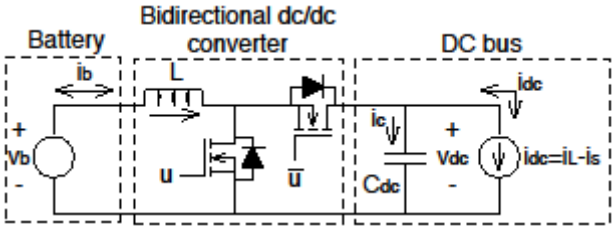

Figure 2: Charger/discharger electrical scheme.

The following sections propose a new control solution based on combining an analog non-linear controller with a digital adaptive controller to ensure a consistent performance in any condition.

Sliding-Mode Current Controller

The first challenge is to design a non-linear controller to ensure global stability of the charger/discharger in any operation condition. This paper proposes to design a Sliding-Mode Controller (SMC) due to its robustness and low sensitivity to parameters variations (Zhao, Qiao, & Ha, March 2014), (Tan, Lai, & Tse, March 2008) and (Sira-Ramírez, Aug 1987). Such characteristics allow to disregard parasitic losses without impacting significantly the validity of the sliding-mode analyses as illustrated in (Bianconi, et al., March 2013), (Zhao, Qiao, & Ha, March 2014) and (Inthamoussou, Pegueroles-Queralt, & Bianchi, Sept 2013).

The bidirectional condition of the charger/discharge of Figure 2 implies that such a circuit must be analyzed for both positive and negative current flows. From the definition of the converter' output power $P_{dc} = P_L - P_s$, positive battery currents i_b stand for the battery providing power, i.e. boost condition since $v_b < v_{dc}$, while negative battery currents i_b stand for the battery absorbing power, i.e. buck condition.

Boost condition (discharge)

In this condition the battery current i_b flows from the battery to the dc bus. Figure 3 shows the simplified electrical scheme of such an operation condition. The switched differential equations (1) and (2) describe the circuit behavior, where u is the binary control signal of the Mosfets, L represents the inductor value and C_{dc} represents the capacitor value.

$$\frac{di_b}{dt} = \frac{v_b - v_{dc}\cdot(1-u)}{L} \qquad (1)$$

$$\frac{dv_{dc}}{dt} = \frac{i_b\cdot(1-u) - i_{dc}}{C_{dc}} \qquad (2)$$

Then, the inductor current must be controlled to ensure the system stability. Such a controller is designed as an SMC based on the switching function $\Psi_d = i_b - i_{ref}$ and sliding surface $\Phi_d = \{\Psi_d = 0\}$. In such a surface i_{ref} represents the reference value imposed to the inductor current, which in turns ensure an stable behavior. However, to guarantee the correct behavior of the SMC, three conditions must be granted (Sira-Ramírez, Aug 1987) (Tan, Lai, & Tse, March 2008): transversality, reachability and equivalent control.

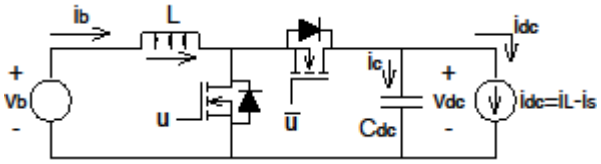

Figure 3: Boost (discharge) condition the charger/discharger.

The transversality condition analyzes the ability of the SMC to affect the system dynamics. This condition is granted if $\frac{d}{du}\left(\frac{d\Psi_d}{dt}\right) \neq 0$ (Sira-Ramírez, Aug 1987). For the boost system (1)-(2) under the control of Φ_d, the time derivative of the switching function is given by (3), and replacing (1) into (3) leads to (4), which confirms the transversality condition.

$$\frac{d\Psi_d}{dt} = \frac{di_b}{dt} \qquad (3)$$

$$\frac{d}{du}\left(\frac{d\Psi_d}{dt}\right) = \frac{v_{dc}}{L} > 0 \qquad (4)$$

The reachability conditions analyze the ability of the SMC to reach the surface. i.e. the desired condition, which in this case is $i_b - i_{ref} = 0$. The reachability conditions depend on the sign of the transversality condition (Sira-Ramírez, Aug 1987), which in this case is positive. Therefore, the reachability conditions to fulfill are:

$$\lim_{\Psi_d \to 0^-} \left.\frac{d\Psi_d}{dt}\right|_{u=1} = \frac{v_b}{L} > 0 \qquad (5)$$

$$\lim_{\Psi_d \to 0^+} \left.\frac{d\Psi_d}{dt}\right|_{u=0} = \frac{v_b - v_{dc}}{L} < 0 \qquad (6)$$

Relations (5) and (6) verify the reachability conditions. Finally, the equivalent control condition establishes that the average value of the binary control signal must be within the signal limits (Sira-Ramírez, Aug 1987). The analysis of the equivalent control is performed within the sliding surface, hence $\Psi_d = 0$ and $\frac{d\Psi_d}{dt} = 0$. Moreover, in dc/dc converters the binary control signal could be $u = 1$ or $u = 0$, hence the equivalent control value u_{eq} must be constrained within $0 < u_{eq} < 1$. Then, replacing u by u_{eq} in (1) and taking into account condition (3), $u_{eq} = 1 - \frac{v_b}{v_{dc}}$. Such an expression leads to relation (7), which verifies the equivalent control condition.

$$0 < u_{eq} < 1 \;\rightarrow\; v_b < v_{dc} < v_{dc} + v_b \qquad (7)$$

In conclusion, since transversality, reachability and equivalent control conditions are fulfilled, the SMC designed with $\Psi_d = i_b - i_{ref} = 0$ is stable. Therefore, under the action of such an SMC, $i_b = i_{ref}$ in any operation condition. An additional analysis required for designing the SMC concerns the implementation law (Tan, Lai, & Tse, March 2008): from the reachability conditions (5) and (6) it is noted that $\Psi_d < 0$ (or $\Psi_d \to 0^-$) requires $u = 1$, while $\Psi_d > 0$ (or $\Psi_d \to 0^+$) requires $u = 0$. Such information will be used afterwards to synthesize the implementation circuit for the SMC.

Buck condition (charge)

In this condition the battery current i_b flows from the dc bus to the battery. Figure 4 shows the simplified electrical scheme with the new current conventions, where the following switched differential equations describe the circuit behavior:

$$\frac{di_b}{dt} = \frac{v_{dc}\cdot(1-u)-v_b}{L} \quad (8)$$

$$\frac{dv_{dc}}{dt} = \frac{i_{dc}-i_b\cdot(1-u)}{C_{dc}} \quad (9)$$

Similar to the boost case, the inductor current must be controlled to ensure system stability. Again, such a controller is designed as an SMC based on the switching function $\Psi_c = i_b - i_{ref}$ and sliding surface $\Phi_c = \{\Psi_c = 0\}$. In this case i_{ref} follows the convention of Figure 4. It must be pointed out that such a current will be negative in the convention of Figure 3. The transversality condition is analyzed from (8)-(9) and (10), which leads to relation (11). Such an expression confirms the transversality condition.

$$\frac{d\Psi_c}{dt} = \frac{di_b}{dt} \quad (10)$$

$$\frac{d}{du}\left(\frac{d\Psi_c}{dt}\right) = -\frac{v_{dc}}{L} < 0 \quad (11)$$

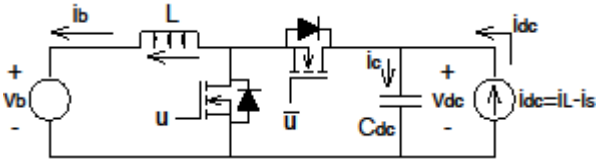

Figure 4: Buck (charge) condition the charger/discharger.

The reachability conditions for $\Psi_c = 0$, defined by the negative value of the transversality condition, are verified in (12) and (13).

$$\lim_{\Psi_c\to 0^-} \frac{d\Psi_c}{dt}\Big|_{u=1} = -\frac{v_b}{L} < 0 \quad (12)$$

$$\lim_{\Psi_c\to 0^+} \frac{d\Psi_c}{dt}\Big|_{u=0} = \frac{v_{dc}-v_b}{L} > 0 \quad (13)$$

Finally, the equivalent control is analyzed for $\Psi_c = 0$ and $\frac{d\Psi_c}{dt} = 0$. Then, replacing u by u_{eq} in (8), (9) and (10), u_{eq} is obtained as in (14), which verifies the equivalent control.

$$0 < u_{eq} = 1 - \frac{v_b}{v_{dc}} < 1 \;\rightarrow\; v_b < v_{dc} < v_{dc} + v_b \quad (14)$$

Again, the SMC designed with $\Psi_c = i_b - i_{ref} = 0$ is stable and it ensures $i_b = i_{ref}$ in any operation condition. From the reachability conditions (12) and (13) it is noted that $\Psi_c < 0$ (or $\Psi_c \to 0^-$) requires $u = 1$, while $\Psi_c > 0$ (or $\Psi_c \to 0^+$) requires $u = 0$. Such conditions are the same ones obtained in the boost condition, which will be used for the design SMC implementation circuit.

SMC implementation

Taking into account that both switching laws of boost and buck cases are the same ($u = 1$ if $\Psi_{c,d} < 0$ and $u = 0$ if $\Psi_{c,d} > 0$), a single unified SMC circuit can be designed to control both cases. To implement both SMC the current conventions in Figure 3 are used: the sliding surface of the buck condition $\Psi_c = i_b - i_{ref} = 0$ is rewritten as $-i_b = -i_{ref}$ while the sliding surface of the boost condition is expressed as $i_b = i_{ref}$. With such an unified convention, positive values of i_{ref} will impose positive battery currents, i.e. discharge the battery, while negative values of i_{ref} will impose negative battery currents, i.e. charge the battery.

In addition, to avoid infinite (and impractical) switching frequencies for the SMC circuit, an hysteresis band $2H$ is added to the surface as explained in (Tan, Lai, & Tse, March 2008). In such a way, the practical switching law becomes:

$$u = 1 \quad \text{if} \quad \Psi_{c,d} \le -H \quad (15)$$

$$u = 0 \quad \text{if} \quad \Psi_{c,d} \ge H \quad (16)$$

With the previous switching law the battery current will be constrained within $i_{ref} - H \le i_b \le i_{ref} + H$ for any operation condition. The hysteresis band $2H$ is defined following physical constraints: limit the switching frequency, limit the inductor current ripple, among others (Tan, Lai, & Tse, March 2008). The switching laws (15) and (16) are implemented in the hybrid analog/digital circuit of Figure 5. The circuit at the left implements exactly such inequalities: if $\Psi_{c,d} \le -H$ the Set input of the Flip-Flop is triggered, which sets the Flip-Flop output $Q = u = 1$; while if $\Psi_{c,d} \ge H$ the Reset input of the Flip-Flop is triggered to reset the Flip-Flop output $Q = u = 0$. A more practical circuit is presented at the right side of the figure, in which the switching law is rewritten as (17) and (18).

$$u = 1 \quad \text{if} \quad i_b \le i_{ref} - H \quad (17)$$

$$u = 0 \quad \text{if} \quad i_b \ge i_{ref} + H \quad (18)$$

Then, the implementation circuit of the right side of Figure 5 measures the battery current and hysteresis band limits to produce the Mosfet activation signals u and $\bar{u}$.

Finally, the previously designed SMC guarantees the system stability in any operation condition by ensuring the condition $i_b = i_{ref}$. The following section presents the design of an adaptive controller to define i_{ref}.

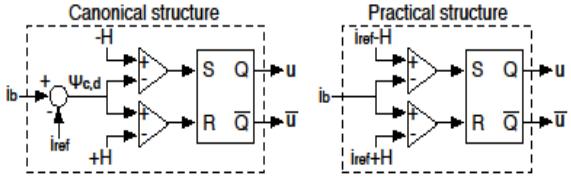

Figure 5: Implementation circuits for the SMC.

EMS Voltage Controller

Taking into account the inductor current control performed by the SMC, the circuital scheme of the charger/discharger can be modeled as in Figure 6, where the inductor and Mosfets are represented by a current source. Such a model is accurate since the inductor current is controlled, hence it behaves as a current source with $i_b = i_{ref}$. The main discrepancy concerns the effect of the horizontal Mosfet operation on the current delivered to the dc bus. Therefore, the current source receives the command i_{ref} but delivers the horizontal Mosfet current i_{MosH}. Since the horizontal Mosfet is active for $u = 0$ (or $\bar{u} = 1$), the average current of such a Mosfet is given by (19), where $d = 1 - \frac{v_b}{v_{dc}}$ represents the converter duty cycle and $d' = 1 - d$ represents the complementary duty cycle. Therefore, the current source model includes a variable gain equal to d'.

$$i_{MosH} = d' \cdot i_b = d' \cdot i_{ref} \quad (19)$$

The mathematical model describing the behavior of dc bus voltage, obtained from Kirchhoff laws and Laplace transform, is given in (20); while the transfer function between such a voltage and the reference current of the SMC is given in (21).

$$V_{dc}(s) = \frac{1}{C_{dc}\cdot s}\cdot\left(d'\cdot I_{ref}(s) - I_{dc}(s)\right) \quad (20)$$

$$Gv_{/i}(s) = \frac{V_{dc}(s)}{I_{ref}(s)} = \frac{d'}{C_{dc}\cdot s} \quad (21)$$

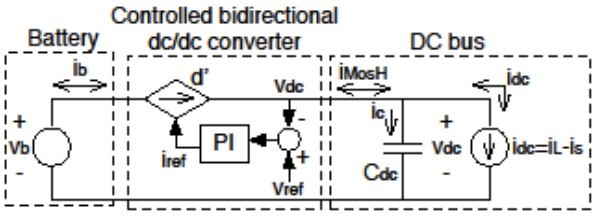

Figure 6: Charger/discharger model including the SMC and voltage controller.

An additional voltage controller is required to regulate the bus voltage, i.e. to provide a stable voltage v_{ref} to the load. This paper considers the design of a PI controller, given in (22), but any other structure could be adopted. Then, the closed loop transfer function between the bus voltage and the desired reference voltage is given by (23).

$$PI(s) = k_p + \frac{k_i}{s} \qquad (22)$$

$$\frac{V_{dc}(s)}{V_{ref}(s)} = \frac{\left(\frac{d'}{C_{dc}}\right)\cdot(k_p\cdot s+k_i)}{s^2+\left(\frac{d'}{C_{dc}}\right)\cdot k_p\cdot s+\left(\frac{d'}{C_{dc}}\right)\cdot k_i} \qquad (23)$$

From the denominator analysis of (23), and from the classical dynamic behavior of second order systems (Ramos-Paja, González, & Saavedra-Montes, Accurate calculation of settling time in second order systems: A photovoltaic application, March 2013), the expressions given in (24) are obtained. In such expression t_s, ρ and ω_n represent the settling-time, damping ration and natural frequency of the dc voltage, respectively.

$$t_s = \frac{3.9}{\rho\cdot\omega_n}, \qquad \rho\cdot\omega_n = \frac{d'\cdot k_p}{2\cdot C_{dc}}, \qquad \omega_n^2 = \frac{d'\cdot k_i}{C_{dc}} \qquad (24)$$

Then, k_p and k_i are calculated from (24) to guarantee the desired dynamic behavior of the bus voltage, i.e. t_s and ρ:

$$k_p = \frac{7.8\cdot C_{dc}}{d'\cdot t_s}, \qquad k_i = \frac{d'\cdot k_p^2}{4\cdot C_{dc}\cdot\rho^2} \qquad (25)$$

Since the complementary duty cycle d' changes with the operation conditions, i.e. bus and battery voltages, such k_p and k_i parameters must to be adapted. Therefore, the adaptive PI controller must to measure the battery and bus voltages to modify k_p and k_i, i.e. vector [Par] in Figure 1, according to the adaptive law imposed by (25). The implementation of the voltage controller is performed using a digital processor to simplify the adaptive law calculation. In such a way, Figure 7 presents the proposed block diagram: the bus and battery voltages are acquired using Analog-to-Digital Converters (ADC), which are available in many Digital Signal Controllers (DSC), such data is processed by the adaptive law to tune the PI parameters. Such a PI controller is a discretized version of (22) based on the bilinear transformation. Finally, the limits of the hysteresis band are calculated and imposed to the SMC circuit (Figure 5) using two Digital-to-Analog Converters (DAC).

Control System Performance

The scheme of Figure 1 was implemented in the power electronics simulator PSIM, which is a standard for dc/dc converters simulation (Ramos-Paja, et al., June 2010) (Femia, Petrone, Spagnuolo, & Vitelli, July 2005) (Bianconi, et al., March 2013). The charger/discharge (Figure 2) was controlled using the hybrid linear/non-linear controller formed by the SMC circuit described in Figure 5 and the adaptive PI controller described in Figure 7. To illustrate the control system performance the following parameters were adopted: $L = 100\ \mu H$, $C_{dc} = 100\ \mu F$, $v_b = 12\ V$ and a required load voltage $v_{ref} = 48\ V$. In addition, the hysteresis band was set to $H = 1\ A$ to ensure a switching frequency around $50\ kHz$. The ADC and DAC were simulated by quantization blocks of 12 bits with a sampling time of $100\ kHz$. Moreover, the adaptive law and digital PI controller were executed using a C-block to simulate the digital processor. Finally, the performance parameters were set as $t_s = 3\ ms$ and $\rho = 0.707$.

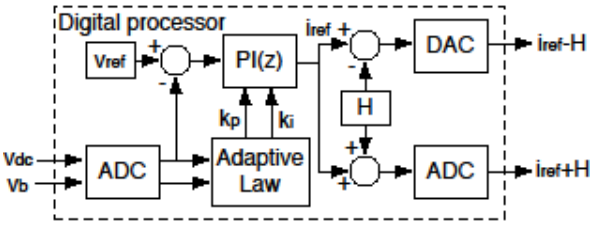

Figure 7: Block diagram of the adaptive digital controller for vdc.

The simulation considers the pulsating load profile depicted in Figure 8: the load current i_Q is $8\ A$ up to $15\ ms$, at that instant i_Q changes to $4\ A$. Moreover, the renewable generator produces a power profile (depicted in terms of the generator current is) that changes due to the environmental, fuel supply and MPPT operation. For example, up to $5\ ms$ the generator produces enough power to supply the load, but at $5\ ms$ the power production is reduced, which forces the charger/discharger to extract power from the battery (depicted in terms of the battery current i_b) to supply the load. The bus current i_{dc} is the difference between the current requested by the load and the current supplied by the source.

Similarly, at $15\ ms$ the generator produces power in excess due to an instantaneous load change, which forces the charger/discharger to store the remaining power into the battery, i.e. negative i_b current. Finally, at $26\ ms$, the battery voltage starts to oscillate to simulate an additional perturbation.

The simulations results, presented in Figure 8, show a satisfactory performance of the control system: the bus voltage v_{dc} is accurately regulated under all the perturbations for both charge and discharge conditions. Moreover, the satisfactory performance of the SMC is also verified, i.e. $i_b = i_{ref}$, even under a strong perturbation on v_b. Finally, Figure 8 also reports the evolution of k_p and k_i, which put in evidence the requirement of the adaptive law to guarantee the desired dynamic performance, i.e. $t_s = 3\ ms$ and $\rho = 0.707$.

Finally, it must be point out that any other dc/dc converter parameters, or performance parameters values, could be defined since the adaptive law will adjust the PI controller.

Conclusions

The paper has presented a EMS for an electric system composed by a renewable DC source, a battery and a load bus. This system was based on a battery charger/discharger controlled to regulate the DC bus voltage. The proposed solution was based on two cascade controllers for the charger/discharger: an adaptive controller designed to regulate the voltage of the DC bus accounting for changes of the model parameters, and a non-linear controller designed to regulate the battery current. This non-linear controller is based on the sliding-mode theory to guarantee the system stability in any operation condition.

Finally, a future improvement of this work consist in including the voltage regulation into the sliding surface to perform a more precise design of the converter dynamics, accounting for the

battery charge/discharge profile, and including the battery state of charge (SOC) regulation.

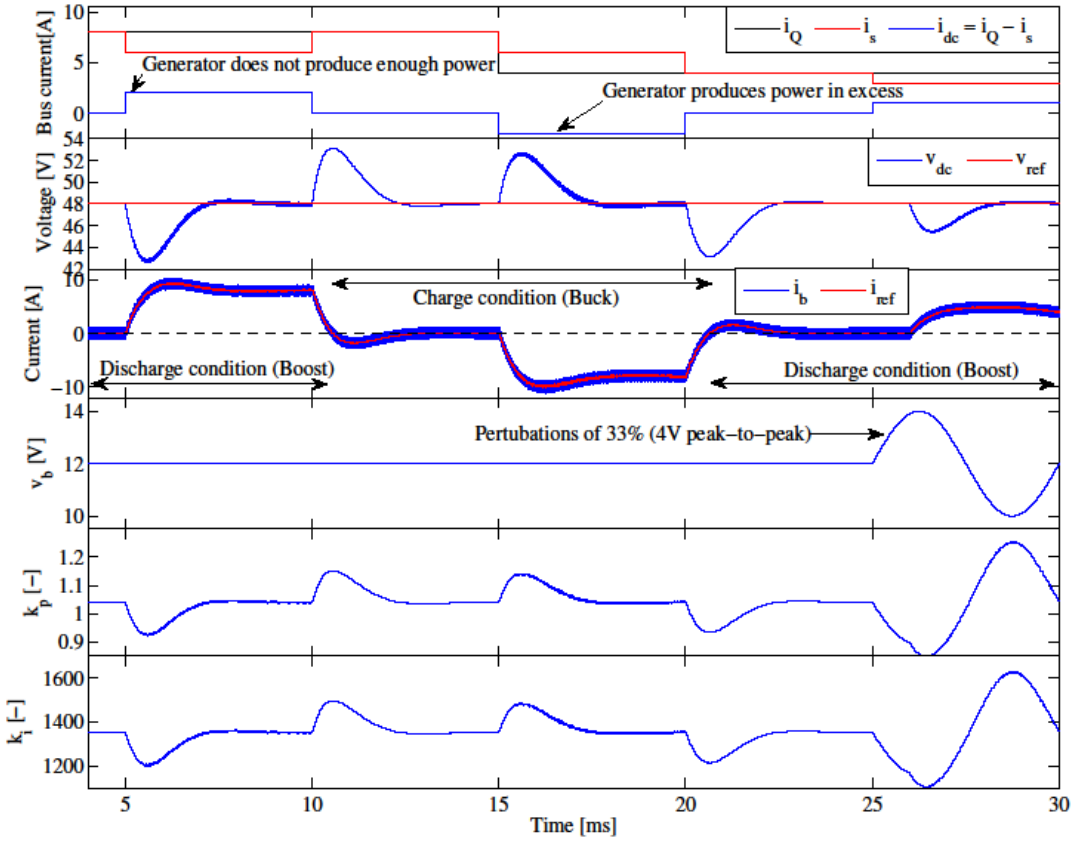

Figure 8: Simulation of the EMS under load and battery perturbations.

Acknowledgment

This paper was supported by Universidad Nacional de Colombia, Instituto Tecnológico Metropolitano and COLCIENCIAS under the projects FC-121056236765, RECONFOP- 21386 (Jóvenes Investigadores-2013), P14215 and P14220, and the doctoral scholarship 012-567.

Bibliografía

Bianconi, E., Calvente, J., Giral, R., Mamarelis, E., Petrone, G., Ramos-Paja, C., . . . Vitelli, M. (March 2013). A fast current-based mppt technique employing sliding mode control. *IEEE Transactions on Industrial Electronics, 60*, 1168-1178.

Bizon, N., Oproescu, M., & Raceanu, M. (Jan 2015). Efficient energy control strategies for a standalone renewable/fuel cell hybrid power source. *Energy Conversion and Management, 90*, 93-110.

Chen, H. S. (May 2014). A study on green consumer intention of portable hydrogen fuel cells. *Energy Education Science and Technology Part A: Energy Science and Research, 32*, 2027-2036.

Femia, N., Petrone, G., Spagnuolo, G., & Vitelli, M. (July 2005). Optimization of perturb and observe maximum power point tracking method. *IEEE Transactions on Power Electronics, 20*, 963-973.

Inthamoussou, F. A., Pegueroles-Queralt, J., & Bianchi, F. D. (Sept 2013). Control of a supercapacitor energy storage system for microgrid applications. *IEEE transactions on energy conversion, 28*, 690-697.

Jang, M., & Agelidis, V. (May 2011). A minimum power-processing-stage fuel-cell energy system based on a boost-inverter with a bidirectional backup battery storage. *IEEE Transactions on Power Electronics, 26*, 1568-1577.

Ramos-Paja, C., Bordons, C., Romero, A., Giral, R., & Martínez-Salamero, L. (March 2009). Minimum fuel consumption strategy for pem fuel cells. *IEEE Transactions on Industrial Electronics, 56*, 685-696.

Ramos-Paja, C., Giral, R., Martínez-Salamero, L., Romano, J., Romero, A., & Spagnuolo, G. (June 2010). A pem fuel-cell model featuring oxygen-excess-ratio estimation and power-electronics interaction. *IEEE Transactions on Industrial Electronics, 57*, 1914–1924.

Ramos-Paja, C., Spagnuolo, G., Petrone, G., & Mamarelis, E. (April 2014). A perturbation strategy for fuel consumption minimization in polymer electrolyte membrane fuel cells: Analysis, design and fpga implementation. *Applied Energy, 119*, 21-32.

Romero-Cadaval, E., Spagnuolo, G., Franquelo, L. G., Ramos-Paja, C., Suntio, T., & Xiao, W. (Sept 2013). Grid-connected photovoltaic generation plants: Components and operation. *IEEE Industrial Electronics Magazine, 7*, 6-20.

Sira-Ramírez, H. (Aug 1987). Sliding motions in bilinear switched networks. *IEEE Transactions on Circuits and Systems, 34*, 919-933.

Sun, K., Zhang, L., Xing, Y., & Guerrero, J. (Oct 2011). A distributed control strategy based on dc bus signaling for modular photovoltaic generation systems with battery energy storage. *IEEE Transactions on Power Electronics, 26*, 3032–3045.

Tan, S. C., Lai, Y., & Tse, C. (March 2008). General design issues of sliding-mode controllers in dc-dc converters. *IEEE Transactions on Industrial Electronics, 55*, 1160-1174.

Zhao, Y., Qiao, W., & Ha, D. (March 2014). A sliding-mode duty-ratio controller for dc/dc buck converters with constant power loads. *IEEE transactions on industry applications, 50*, 1448-1458.